Available online at www.sciencedirect.com
ScienceDirect
Ceramics International 40 (2014) 1561–1567
CERAMICS INTERNATIONAL
www.elsevier.com/locate/ceramint

A two-step solid state synthesis of $LiFePO_4$/C cathode with varying carbon contents for Li-ion batteries

Jihyeon Gim, Jinju Song, Diem Nguyen, Muhammad Hilmy Alfaruqi, Sungjin Kim, Jungwon Kang, Alok Kumar Rai, Vinod Mathew, Jaekook Kim*

Department of Materials Science and Engineering, Chonnam National University, 300 Yongbong-dong, Bukgu, Gwangju 500-757, South Korea

Received 13 June 2013; received in revised form 8 July 2013; accepted 8 July 2013
Available online 15 July 2013

Abstract

Olivine structured $LiFePO_4$/carbon composites with different amounts of carbon were prepared by a modified two-step solid-state reaction. The iron citrate used as both iron and carbon sources in the reaction resulted in the formation of carbon coatings on the olivine particles as the mixed precursors were heated at three different initial-step temperatures of 200, 300 and 400 °C followed by a second-step annealing at moderate temperatures of 700 °C. The obtained final powders with varying carbon contents were systematically analyzed by characterization techniques of thermo-gravimetric analysis, X-ray powder diffraction, field-emission scanning electron microscopy, and field-emission transmission electron microscopy prior to electrochemical testing in order to determine the structural and calcination effects on the electrochemical properties of the composites. The field-emission transmission electron microscopy images revealed that the morphology of the $LiFePO_4$ composites consist of agglomerated particles surrounded by carbon as a conductive material. Among the prepared samples, the $LiFePO_4$/carbon composite calcined at initial-step temperature of 300 °C showed the highest discharge capacity and the best rate capability in the voltage range of 2.5–4.2 V.

Keywords: Lithium iron phosphate; Cathode materials; Solid-state synthesis; Lithium-ion batteries

1. Introduction

Rechargeable Li-ion batteries are considered as an attractive power source for a variety of applications including cellular phones, notebook computers, camcorders and even electric vehicles. Although $LiCoO_2$ is currently the most widely applied cathode material in commercial lithium-ion batteries owing to its decent electrochemical properties and convenience of preparation, it is not free from disadvantages of low practical capacity, high cost, toxicity and inferior safety features [1,2]. In recent years, NASICON or olivine-type materials built from MO_6 octahedron (where M is Fe, Co, Mn, Ni, V or Ti) and strongly covalent bonded tetrahedral polyanions (XO_4^{n-}, where X is P, W, S or Mo), have been investigated as cathodes with significant structural stability [3–6]. Among these, $LiFePO_4$ remains a promising candidate due to its high theoretical capacity (170 mA h g^{-1}) [2], low cost [7,8], environmental benignity [9], good cycle life properties [10–15], excellent thermal stability [16,17], and an approximately flat voltage plateau around 3.4–3.5 V versus lithium. Despite its merits, $LiFePO_4$ suffers from rate-limiting characteristics of low electronic conductivity ($\leq 10^{-9}$ S cm^{-1}) [18] and lithium ion diffusivity that hinders the practical application of this olivine as Li-ion battery cathodes. Consequently, tremendous efforts are aimed at minimizing the intrinsic disadvantages and improving the electrochemical properties of $LiFePO_4$ using various strategies such as reducing particle sizes [19,20], aliovalent cation substitution [18], particle morphology tailoring [21–23] and developing composites or performing particle coatings with conductive materials [24–29].

Carbon coating on particle surfaces as well as designing carbon-contained composites has been recognized as one of the most effective way to improve the rate capabilities in $LiFePO_4$. Hsu et al. reported that nanosized $LiFePO_4$/carbon composites (noted hereafter as LFP/C) were successfully

---

*Corresponding author. Tel.: +82 62 530 1703; fax: +82 62 530 1699.
E-mail address: jaekook@chonnam.ac.kr (J. Kim).

0272-8842/$ - see front matter © 2013 Elsevier Ltd and Techna Group S.r.l. All rights reserved.
http://dx.doi.org/10.1016/j.ceramint.2013.07.043

synthesized by a sol–gel method using citric acid as a chelating agent and a carbon source [25]. The reversible capacities for the LFP/C cathode obtained were 148 and 125 mA h g^{-1} at C-rates of 0.025 and 0.1C respectively. Dominko et al. investigated the dependency of varying carbon content on carbon layer thickness formed on the LFP/C nanoparticles via a sol–gel technique by controlling the amount of Hydroxyethylcellulose (HEC) used as a carbon source during synthesis [26]. This study reported that LFP/C with 3.2 wt% carbon content and 1–2 nm thick carbon coating displayed a reversible capacity of about 116 mA h g^{-1} at 5C rate. Nien et al. used a co-precipitation method utilizing a polymer precursor (polystyrene) to develop an LFP/C cathode that demonstrated less than 110 mA h g^{-1} of capacity under 0.5C rate condition [27]. Contrary to solution synthetic routes, the conventional solid-state reaction permits the opportunity for multi-step heat treatments to not only eliminate organic materials but also serves as a prospective approach to introduce carbon sources such as sucrose, glucose or polymer precursors that can directly contribute to surface conducting layers on the formed crystalline particles. Since the approach of forming surface coatings is relatively easier than that followed in solution methods, the strategy to produce high-power performance LFP/C composites by simple solid-state reactions without any complicated separation procedures remains significant.

In this work, we demonstrate an effective method to control the thickness of an in-situ surface carbon layer formed on the LFP/C composites via a modified solid-state reaction method. The high temperature reaction uses iron citrate, which acts as a dual source of iron as well as carbon, as one of the starting materials. The main focus on this work has been to study the effect of heat treatment on the residual carbon content and the carbon coating layer formed on the prepared particles. In addition, the present study also investigates the influence of the heating process on particle formation by a coherent understanding obtained from thermo-gravimetric, elemental, morphological and electrochemical analyses.

2. Experimental

2.1. Material synthesis

LFP/C composites were prepared by the solid state reaction method using lithium carbonate (Li_2CO_3, 98% Daejung), iron (III) citrate hydrated ($FeC_6H_5O_7 \cdot xH_2O$, 98% Aldrich) and ammonium dihydrogen phosphate ($NH_4H_2PO_4$, 99% Junsei) as the starting materials. In brief, 0.01 mol Li_2CO_3, 0.02 mol iron citrate, and 0.02 mol $NH_4H_2PO_4$ corresponding to 0.02 mol of $LiFePO_4$ was thoroughly milled in an acetone medium using the conventional ball milling apparatus with a rotation speed of about 120 rpm for 24 h. The resultant material was divided into three parts, which were pre-heated at three different temperatures, viz. 200, 300 and 400 °C for 3 h in air. Subsequently, all the heated samples were ground again and then annealed at 700 °C for 6 h under argon (Ar) atmosphere and the final products are marked as LFP/C-200, LFP/C-300 and LFP/C-400 respectively.

2.2. Material characterization

The thermal decomposition behavior of the annealed samples was examined with a thermo-gravimetric analyzer (TGA) (TA instruments SDT Q-600) at a scanning rate of 5 °C min^{-1} from room temperature to 800 °C under air flow of 100 mL min^{-1}. The structure and morphology of the prepared powders were identified by X-ray diffraction (XRD) using a Shimadzu X-ray diffractometer with Cu Kα radiation ($\lambda = 1.5406$ Å), field-emission scanning electron microscopy (FE-SEM, S-4700 Hitachi) and high-resolution transmission electron microscopy (HR-TEM, Philips Tecnai F20 at 200 kV). The obtained powders were ultrasonically dispersed in ethanol, dropped onto TEM grids and allowed to evaporate residual solvent in air at room temperature before obtaining TEM images. Elemental analysis was carried out using a Flash-2000 Thermo Fisher model to determine the practical amount of carbon in the annealed LFP/C composites.

2.3. Electrochemical measurements

The working electrode was prepared by mixing the active material with 10 wt% of Ketjen black as a conductive reagent and 15 wt% of polytetrafluoroethylene (PTFE) as a binder. The mixture was pressed onto a stainless steel mesh and vacuum dried at 120 °C for 12 h to eliminate residual moisture. A 2032 coin-type cell was fabricated using the lithium metal as a counter electrode, separated by a polymer membrane (Celgard 2400) and subsequently stored for 12 h in a glove box before the electrochemical measurements. The electrolyte employed was a solution of 1 M $LiPF_6$ in a mixture of ethylene carbonate/dimethyl carbonate (EC/DMC) with 1:1 volume ratio. The galvanostatic tests were carried out with a programmable battery tester (NAGANO, BTS-2400H) at a constant current of 28.9 mA g^{-1} (=0.17 C) and C-rate performances were evaluated at different currents by cycling them for three times at each rate in the potential range of 2.5–4.2 V versus lithium.

3. Results and discussion

3.1. Characterization of structure and morphology

Thermo-gravimetric and differential thermal analysis (TG/DTA) were used to determine the reaction temperatures for the synthesis of the LFP/C composites. The TG/DTA curves observed under air atmosphere for the ball-milled mixture of starting precursors namely, Li_2CO_3, $FeC_6H_5O_7 \cdot xH_2O$ and $NH_4H_2PO_4$ are displayed in Fig. 1(a). There are several stages of weight loss regions in the TG plot that are reflected as corresponding endothermic and exothermic peaks in the DTA plot. The first domain is attributed to the release of physically absorbed water at temperatures below 200 °C. The second temperature domain ranging from 200 to 450 °C shows continuous and steep weight loss and may be ascribed to the decomposition of carbonate and organo-phosphonates. Hence, temperatures of 200, 300, and 400 °C were selected for pre-heat treatments to determine control over the lasting residual carbon content. Finally, the third region indicating significant weight loss displays a strong exothermic peak at 490 °C, which may be ascribed to the decomposition of the remaining reactants and the crystallization of $LiFePO_4$ [25,30,31]. At temperatures above 800 °C, no obvious exothermic/endothermic reaction or weight-loss appears thereby indicating the completion of the entire reaction. Therefore, final or a second-step heat treatment at temperatures of 700 °C was identified to obtain LFP/C composites with high crystallinity.

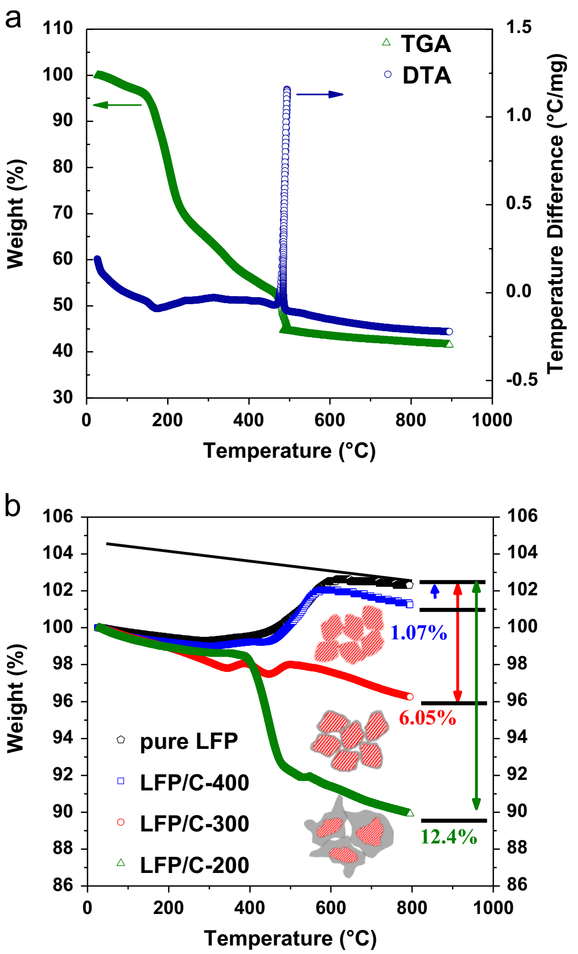

Fig. 1. (a) TG/DTA curves for precursor (the mixture of Li_2CO_3, $FeC_6H_5O_7 \cdot xH_2O$ and $NH_4H_2PO_4$) after ball-milling in air atmosphere, (b) TG curves for the LFP/C-200, LFP/C-300 and LFP/C-400 composites formed by initial pre-heating at 200, 300 and 400 °C, respectively in air atmosphere and subsequent calcination at 700 °C in Argon atmosphere compared with that of pure $LiFePO_4$.

The carbon contents in the LFP/C composites were estimated by comparative analysis of the TG curves of the LFP/C-200, LFP/C-300 and LFP/C-400 composites and that of pure $LiFePO_4$. The difference between the final points observed in the TG plots of the LFP/C composites and pure $LiFePO_4$ may correspond to the carbon content in the composites assuming that the residual carbon in the composites is burned off by heating in air at 800 °C. It can be easily interpreted from the TG plot of pure $LiFePO_4$ in Fig. 1(b) that a weight gain of approximately 4.6 wt%, which is obtained by extrapolation of this curve, is comparable to the theoretical value of 4–5 wt% afforded by the complete oxidation of Fe^{2+} to Fe^{3+} [31,32]. The estimated residual carbon in the case of LFP/C-200 with respect to that of pure $LiFePO_4$ was the highest (12.4 wt%), as shown in the plot of Fig. 1(b). In addition, the weight difference of LFP/C-300 is relatively lower, viz. 6.05 wt% when compared to that for LFP/C-200. However, the weight loss difference calculated by comparing the TG plot of LFP/C-400 and pure $LiFePO_4$ is only 1.07%, suggesting that the level of carbon formation is the lowest among that for the prepared composites. Schematic figures are also given in the TG plot with respect to the carbon coating tendency on the particles. The results of the elemental analysis performed to determine the carbon contents in the samples are summarized in Table 1. The calculated percentages of carbon in the annealed composites, viz., LFP/C-200, LFP/C-300 and LFP/C-400 composites are 9.206, 3.176 and 0.838 wt%, respectively. As anticipated, the highest percentage of carbon is observed in the LFP/C-200 composite, which might be due to the incomplete decomposition of the organo–metallic complex. The value of carbon contents obtained from elemental analysis indicated a similar tendency to that of the TG data. Hence, the anticipation of carbon contents from TG analysis may tend to be quite reasonable (detailed discussion in the TEM part).

Fig. 2 shows the X-Ray diffraction patterns of the LFP/C-200, LFP/C-300 and LFP/C-400 composites. The XRD peaks of all of the composites demonstrate the formation of highly crystalline $LiFePO_4$ phase with an ordered olivine structure indexed to the orthorhombic *Pnma* space group devoid of any detectable impurity phases. The lattice parameters for the LFP/C composites are given in Table 1 and the values of results are very close to the standard data ($a = 10.334$ Å, $b = 6.010$ Å, and $c = 4.693$ Å) given by JCPDS 83-2092 [33]. The surface morphologies of the LFP/C-200, LFP/C-300 and LFP/C-400 composites were characterized by FE-SEM and the results are shown in Fig. 3(a)–(c). The SEM images of all the composites

Table 1
Lattice parameters, unit cell volume values, and carbon contents from elemental analysis of LFP/C-200, LFP/C-300 and LFP/C-400 composites.

Sample name	***a*** **(Å)**	***b*** **(Å)**	***c*** **(Å)**	**Cell volume ($Å^3$)**	**Carbon content (wt%)**
LFP/C-200	10.3333	6.0103	4.6912	291.3546	9.206
LFP/C-300	10.3300	6.0073	4.6895	291.0087	3.176
LFP/C-400	10.3280	6.0129	4.6919	291.3770	0.838

are similar and the particles appear to have sub-micrometer or micrometer sizes with irregular shapes and severe agglomeration. The $LiFePO_4$ particle-sizes are observed to range between 1 and 2 µm. Prosini et al. [34] reported that particle size decreases as the amount of carbon increases by impeding the diffusion during heat-treatment. It is well known that tailoring the particle morphology in solid state synthesis is quite complicated because of the high heating temperatures, which results in irregular particle morphology and unexpected aggregation.

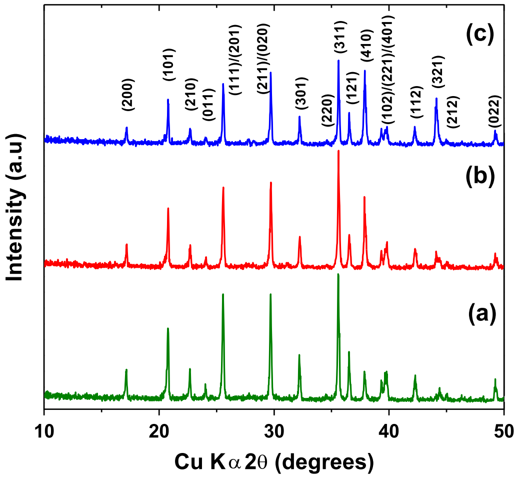

Fig. 2. XRD patterns of (a) LFP/C-200, (b) LFP/C-300 and (c) LFP/C-400 composites prepared by a two-step solid state reaction.

In order to observe carbon formations in the prepared composites, HR-TEM investigations were performed and the results are shown in Fig. 3(d)–(f). Carbon distribution on the $LiFePO_4$ particle surface was observed to be specific for each of these samples. As anticipated, the TEM picture of LFP/C-200, in Fig. 3(d), distinctly shows large amount of carbon formation around the particles. The dark gray region shows the $LiFePO_4$ particles while the light gray region shows the carbon on the surface. The observation of large carbon formation may be attributed to the apparently lesser decomposition of organic matters that originated from the low pre-calcination temperature of 200 °C. The HR-TEM image of the LFP/C-300 sample shown in Fig. 3(e) clearly reveals that the carbon layer on the surface of the $LiFePO_4$ particles has a thickness of about 7 nm and thereby indicates that this appropriate carbon formation can make positive contribution to its electrochemical properties. This claim is coincident with the finding by Dominko et al. that the presence of surface conductive coating layers of thickness less than 10 nm significantly influenced the electrode performance of LFP [26]. Further, Cho et al. also identified

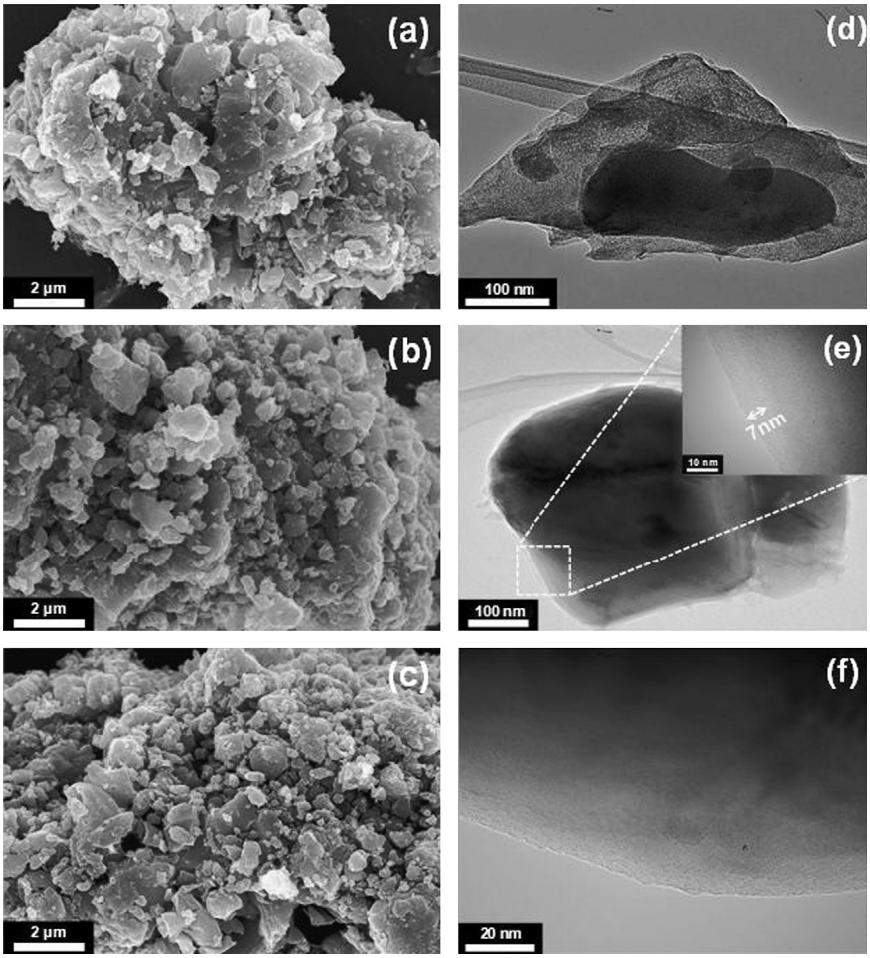

Fig. 3. FE-SEM images of (a) LFP/C-200, (b) LFP/C-300 and (c) LFP/C-400 composites with different carbon contents and corresponding HR-TEM images showing the carbon covered particles in the (d) LFP/C-200, (e) LFP/C-300 and (f) LFP/C-400 composites and indicating the formation of the carbon layer.

that uniform carbon coating layer with thickness as low as 4–8 nm facilitated a proper passivation layer for redox reaction and ultimately contributed to improved electrochemical characteristics in LFP [35]. On the other hand, it appears that the carbon coating is not distinguishable in LFP/C-400, as observed in Fig. 3(f). It is also possible that the low carbon content may be insufficient to facilitate a surface coating that is spread over the entire particle surface. According to Wang's results, such a disconnected carbon network can lead to electronic inter-particle connections, but does not block the direct contact between the active particles and the penetrated electrolyte [36].

3.2. Electrochemical performance

The electrochemical performances for the samples as cathodes in lithium test cells were examined by conducting charge–discharge tests. Fig. 4 shows the initial charge and discharge profiles of the LFP/C-200, LFP/C-300 and LFP/C-400 composites in the voltage range of 2.5–4.2 V at a current density of 28.9 mA g^{-1} corresponding to 0.17 C. The resultant specific capacities were calculated based on solely for the mass of pure $LiFePO_4$. The first discharge capacities of LFP/C-200, LFP/C-300 and LFP/C-400 are 154, 160 and 131 mA h g^{-1}, respectively, corresponding to 91%, 94% and 77% of theoretical capacity values (170 mA h g^{-1}). A flat discharge profile was observed over a wide potential range at 3.4 V, indicating the two-phase nature of the lithium extraction and insertion reactions between $LiFePO_4$ and $FePO_4$ [2]. It is interesting to notice that the optimized pre-heating temperature to form a carbon layer of sufficient thickness on the $LiFePO_4$ particle is 300 °C based on the aforementioned results of various analyses. The uniformed coating layer may facilitate an enhancement in the contact between the conducting additive and active materials. Further, the nanoscale thickness of the coating may also not hinder the diffusion of Li-ions through the particle surface. The aforesaid reasons may thus contribute to the better electrochemical performance of the LFP/C-300 sample. On the other hand, the lower value of the discharge capacity of the LFP/C-200 and LFP/C-400 composites could be related to their relatively thick carbon coatings and larger particle size with less carbon coating, respectively.

Fig. 5 shows the rate performances of the LFP/C-200, LFP/C-300 and LFP/C-400 composite cathodes at 0.17–11 C rates cycled three times at each rate. Among these, the LFP/C-300 composite displayed a longer plateau and the best rate performances of 101 mA h g^{-1} even at current densities as high as 11 C, possibly due to the uniform carbon coating layer of 7 nm thickness, which appears to be sufficient for the supply of electrons to the electrochemically active sites at the particle surface. However, the LFP/C-200 composite showed a fairly low discharge capacity of 88 mA h g^{-1} at the same current rate of 11 C. It is assumed that as the carbon coating becomes thicker, the pores become less permeable to the electrolyte solution [26]. Of course, if the penetration of the electrolyte into the pore system is partially hindered, the surface area available for the lithium ion intercalation/de-intercalation process is consequently lower, which corresponds to a lower specific capacity under a given high rate condition. Further, a thick carbon surface coating may hinder lithium penetration through the particle and lead to lower capacities. Hence the LFP/C-200 cathode may have shown apparently lower electrochemical performance than that displayed by the LFP/C-300 cathode. In comparison to carbon-coated $LiFePO_4$ reported in literature, the values of 160 m Ah g^{-1} displayed by the LFP/C-300 cathode at C/10 and 0.35C rates are still competitive [26,37–41]. Furthermore, the capacity retention of LFP/C-300 cathode under high current densities is quite outstanding, probably due to the moderate carbon content that may tend to improve the electronic conductivity and lithium ion diffusivity. On the other hand, the LFP/C-400 composite showed poorer rate capability than the LFP/C-200 and LFP/C-300 composites at rates of up to 11 C probably due to the absence of carbon coating or due to insufficient carbon for uniform surface coating on LFP particles.

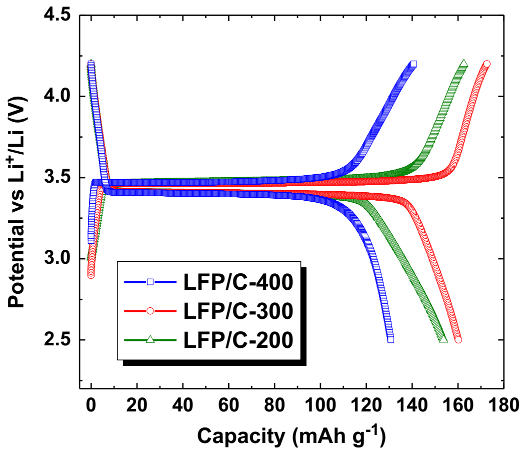

Fig. 4. The first charge and discharge profiles for the LFP/C-200, LFP/C-300 and LFP/C-400 composites at a current density of 28.9 mA g^{-1} (0.17 C) in the voltage range of 2.5–4.2 V.

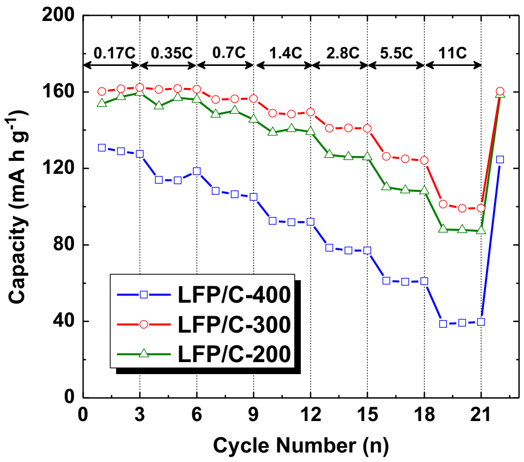

Fig. 5. The C-rate performances of the LFP/C-200, LFP/C-300 and LFP/C-400 composites at different current densities starting from 0.17 C to 11 C.

4. Conclusions

$LiFePO_4$/C composites with different amount of carbon contents were successfully synthesized by a modified two step solid-state reaction without adding any extra carbon source during synthesis. During the preparation of the composites, the initial-step temperatures were chosen between 200 and 400 °C whereas the second step annealing was performed at a common moderated temperature of 700 °C. The present study investigated the effects of pre-heating temperature on the electrochemical behavior of the LFP/C composites. The results showed that controlling the pre-heating temperature influences the generation of in-situ carbon layer thickness and hence improving the performance of the $LiFePO_4$/C cathodes. It is also observed that the thickness and content of the carbon coating can be controlled by choosing the appropriate pre-heat calcination temperature. Increasing the pre-heating temperature leads to a decrease in the carbon content. The amounts of carbon were investigated by elemental analysis and found to be 9.206 wt %, 3.176 wt% and 0.838 wt% for the $LiFePO_4$/carbon composites calcined at 700 °C after pre-heating at 200 °C, 300 °C and 400 °C respectively. The carbon in the $LiFePO_4$/C composites is obtained from the citrate anion which is used as a precursor and a carbon source during the solid-state reaction process. The carbon can suppress the growth of the $LiFePO_4$ particles during the annealing process and enhance the electronic conductivity of the composites. The XRD results showed that the materials had an olivine structure (space group: *Pnma*) and complete crystallization without any impurities. The TEM images also confirmed the carbon coating on the surface of the $LiFePO_4$ particles. Among the prepared composites, the sample pre-heated at 300 °C showed better electrochemical performance. When employed as a cathode in a lithium test cell, LFP/C-300 cathode delivered an initial discharge capacity of $160\ mA\ h\ g^{-1}$ at a current density of $28.9\ mA\ g^{-1}$(0.17 C). Even at a high current density of 11 C, this composite still presents a discharge capacity of $101\ mA\ h\ g^{-1}$ in the voltage range of 2.5–4.2 V versus Li/Li^+ at room temperature. These improved electrochemical performances can be attributed to the uniform carbon coating of 7 nm thickness which may facilitate an enhancement in electronic conduction and also promote lithium ion diffusion. This comparative study reveals the necessity of forming a conductive coating along with particle size reduction for improving the electrochemical properties of $LiFePO_4$ at high C-rates.

Acknowledgments

This work was supported by Priority Research Centers Program through the National Research Foundation of Korea (NRF) funded by the Ministry of Education, Science and Technology (2009-0094055).

References

[1] B. Scrosati, Challenge of portable power, Nature 373 (1995) 557–558.

[2] A.K. Padhi, K.S. Nanjundaswamy, J.B. Goodenough, Phospho-olivines as positive-electrode materials for rechargeable lithium batteries, Journal of the Electrochemical Society 144 (1997) 1188–1194.

[3] A. Yamada, S.C. Chung, K. Hinokuma, Optimized $LiFePO_4$ for lithium battery cathodes, Journal of the Electrochemical Society 148 (2001) A224–A229.

[4] N.N. Bramnik, K. Nikolowski, C. Baehtz, K.G. Bramnik, H. Ehrenberg, Phase transitions occurring upon lithium insertion–extraction of $LiCoPO_4$, Chemistry of Materials 19 (2007) 908–915.

[5] H. Huang, S.C. Yin, T. Kerr, N. Taylor, L.F. Nazar, Nanostructured composites: a high capacity, fast rate $Li_3V_2(PO_4)_3$/carbon cathode for rechargeable lithium batteries, Advanced Materials 14 (2002) 1525–1528.

[6] F. Zhou, M. Cococcioni, K. Kang, G. Ceder, The Li intercalation potential of $LiMPO_4$ and $LiMSiO_4$ olivines with M=Fe, Mn, Co, and Ni, Electrochemistry Communications 6 (2004) 1144–1148.

[7] A.S. Andersson, J.O. Thomas, The source of first-cycle capacity loss in $LiFePO_4$, Journal of Power Sources 97–98 (2001) 498–502.

[8] G. Arnold, J. Garche, R. Hemmer, S. Ströbele, C. Vogler, M. Wohlfahrt-Mehrens, Fine-particle lithium iron phosphate $LiFePO_4$ synthesized by a new low-cost aqueous precipitation technique, Journal of Power Sources 119–121 (2003) 247–251.

[9] C.H. Mi, X.B. Zhao, G.S. Cao, J.P. Tu, In situ synthesis and properties of carbon-coated $LiFePO_4$ as Li-ion battery cathodes, Journal of the Electrochemical Society 152 (2005) A483–A487.

[10] D. Zhang, R. Cai, Y. Zhou, Z. Shao, X.-Z. Liao, Z.-F. Ma, Effect of milling method and time on the properties and electrochemical performance of $LiFePO_4$/C composites prepared by ball milling and thermal treatment, Electrochimica Acta 55 (2010) 2653–2661.

[11] L.S. Gómez, I. de Meatza, M.I. Martín, M. Bengoechea, I. Cantero, M. E. Rabanal, Morphological, structural and electrochemical properties of lithium iron phosphates synthesized by spray pyrolysis, Electrochimica Acta 55 (2010) 2805–2809.

[12] B. Huang, X. Zheng, D. Jia, M. Lu, Design and synthesis of high-rate micron-sized, spherical $LiFePO_4$/C composites containing clusters of nano/microspheres, Electrochimica Acta 55 (2010) 1227–1231.

[13] K. Wang, R. Cai, T. Yuan, X. Yu, R. Ran, Z. Shao, Process investigation, electrochemical characterization and optimization of $LiFePO_4$/C composite from mechanical activation using sucrose as carbon source, Electrochimica Acta 54 (2009) 2861–2868.

[14] M. Gao, Y. Lin, Y. Yin, Y. Liu, H. Pan, Structure optimization and the structural factors for the discharge rate performance of $LiFePO_4$/C cathode materials, Electrochimica Acta 55 (2010) 8043–8050.

[15] J. Xie, N. Imanishi, T. Zhang, A. Hirano, Y. Takeda, O. Yamamoto, Li-ion diffusion kinetics in $LiFePO_4$ thin film prepared by radio frequency magnetron sputtering, Electrochimica Acta 54 (2009) 4631–4637.

[16] D. Wang, X. Wu, Z. Wang, L. Chen, Cracking causing cyclic instability of $LiFePO_4$ cathode material, Journal of Power Sources 140 (2005) 125–128.

[17] A.S. Andersson, J.O. Thomas, B. Kalska, L. Haggstrom, Thermal stability of $LiFePO_4$-based cathodes, Electrochemical and Solid-State Letters 3 (2000) 66–68.

[18] S.-Y. Chung, J.T. Bloking, Y.-M. Chiang, Electronically conductive phospho-olivines as lithium storage electrodes, Nature Materials 1 (2002) 123–128.

[19] M. Gaberscek, R. Dominko, J. Jamnik, Is small particle size more important than carbon coating? An example study on $LiFePO_4$ cathodes, Electrochemistry Communications 9 (2007) 2778–2783.

[20] C. Delacourt, P. Poizot, S. Levasseur, C. Masquelier, Size effects on carbon-free $LiFePO_4$ powders, Electrochemical and Solid-State Letters 9 (2006) A352–A355.

[21] A. Vadivel Murugan, T. Muraliganth, A. Manthiram, Rapid microwave-solvothermal synthesis of phospho-olivine nanorods and their coating with a mixed conducting polymer for lithium ion batteries, Electrochemistry Communications 10 (2008) 903–906.

[22] K. Saravanan, M.V. Reddy, P. Balaya, H. Gong, B.V.R. Chowdari, J. J. Vittal, Storage performance of $LiFePO_4$ nanoplates, Journal of Materials Chemistry 19 (2009) 605–610.

[23] D. Kim, J. Lim, E. Choi, J. Gim, V. Mathew, Y. Paik, H. Jung, W. Lee, D. Ahn, S. Paek, J. Kim, Synthesis of highly crystalline olivine-type $LiFePO_4$ nanoparticles by solution-based reactions, Surface Review and Letters 17 (2010) 111–119.

[24] H. Huang, S.C. Yin, L.F. Nazar, Approaching theoretical capacity of $LiFePO_4$ at room temperature at high rates, Electrochemical and Solid-State Letters 4 (2001) A170–A172.

[25] K.-F. Hsu, S.-Y. Tsay, B.-J. Hwang, Synthesis and characterization of nano-sized $LiFePO_4$ cathode materials prepared by a citric acid-based sol–gel route, Journal of Materials Chemistry 14 (2004) 2690–2695.

[26] R. Dominko, M. Bele, M. Gaberscek, M. Remskar, D. Hanzel, S. Pejovnik, J. Jamnik, Impact of the carbon coating thickness on the electrochemical performance of $LiFePO_4$/C composites, Journal of the Electrochemical Society 152 (3) (2005) A607–A610.

[27] Y.-H. Nien, J.R. Carey, J.-S. Chen, Physical and electrochemical properties of $LiFePO_4$/C composite cathode prepared from various polymer-containing precursors, Journal of Power Sources 193 (2009) 822–827.

[28] G. Hasegawa, Y. Ishihara, K. Kanamori, K. Miyazaki, Y. Yamada, K. Nakanishi, T. Abe, Facile preparation of monolithic $LiFePO_4$/carbon composites with well-defined macropores for a lithium-ion battery, Chemistry of Materials 23 (2011) 5208–5216.

[29] J. Zhang, L. Zhuo, L. Zhang, C. Wu, X. Zhang, L. Wang, Synthesis and electrochemical properties of $LiFePO_4$/C composite cathode material prepared by a new route using supercritical carbon dioxide as a solvent, Journal of Materials Chemistry 21 (2011) 6975–6980.

[30] Y. Hu, M.M. Doeff, R. Kostecki, R. Finones, Electrochemical performance of sol–gel synthesized $LiFePO_4$ in lithium batteries, Journal of the Electrochemical Society 151 (2004) A1279–A1285.

[31] S. Yang, Y. Song, P.Y. Zavalij, M. Stanley Whittingham, Reactivity, stability and electrochemical behavior of lithium iron phosphates, Electrochemistry Communications 4 (3) (2002) 239–244.

[32] A. Kuwahara, S. Suzuki, M. Miyayama, High-rate properties of $LiFePO_4$/carbon composites as cathode materials for lithium-ion batteries, Ceramics International 34 (2008) 863–866.

[33] F. Cheng, W. Wan, Z. Tan, Y. Huang, H. Zhou, J. Chen, X. Zhang, High power performance of nano-$LiFePO_4$/C cathode material synthesized via lauric acid-assisted solid-state reaction, Electrochimica Acta 56 (2011) 2999–3005.

[34] P.P. Prosini, D. Zane, M. Pasquali, Improved electrochemical performance of a $LiFePO_4$-based composite cathode, Electrochimica Acta 46 (2001) 3517–3523.

[35] Y.-D. Cho, G.T.-K. Fey, H.-M. Kao, The effect of carbon coating thickness on the capacity of $LiFePO_4$/C composite cathodes, Journal of Power Sources 189 (2009) 256–262.

[36] Y. Wang, J. Wang, J. Yang, Y. Nuli, High-rate $LiFePO_4$ electrode material synthesized by a novel route from $FePO_4 \cdot 4H_2O$, Advanced Functional Materials 16 (2006) 2135–2140.

[37] J.K. Kim, G. Cheruvally, J.H. Ahn, G.Ch. Hwang, J.B. Choi, Electrochemical properties of carbon-coated $LiFePO_4$ synthesized by a modified mechanical activation process, Journal of Physics and Chemistry of Solids 69 (2008) 2371–2377.

[38] C.H. Mi, G.S. Cao, X.B. Zhao, Low-cost, one-step process for synthesis of carbon-coated $LiFePO_4$ cathode, Materials Letters 59 (2005) 127–130.

[39] H. Liu, P. Zhang, G.C. Li, Q. Wu, Y.P. Wu, $LiFePO_4$/C composites from carbothermal reduction method, Journal of Solid State Electrochemistry 12 (2008) 1011–1015.

[40] M.E. Zhong, Z.T. Zhou, Preparation of high tap-density $LiFePO_4$/C composite cathode materials by carbothermal reduction method using two kinds of Fe^{3+} precursors, Materials Chemistry and Physics 119 (2010) 428–431.

[41] X. Li, W. Wang, C. Shi, H. Wang, Y. Xing, Structural and electrochemical characterization of $LiFePO_4$/C prepared by a sol–gel route with long- and short-chain carbon sources, Journal of Solid State Electrochemistry 13 (2009) 921–926.